FUDMA Journal of Engineering and Technology
ISSN: 3092-9385
https://fjet.fudutsinma.edu.ng/index.php/fjet/
Volume 2, Issue 1, 2026, 59-72

Development and Performance Evaluation of Biomass Pyrolysis System for Biofuel Production

Ndagi MAMUDU[1], Ibrahim S. MOHAMMED[2], Mohammed ALIYU[3], Peter DANIEL[4], Timothy Y. AKANDE[5], Bala A. GARBA[6]

[1*,2,3,4,5]Department of Agricultural and Bio-Resources Engineering, Federal University of Technology, Minna, Nigeria
[6]Department of Mechanical Engineering, Federal University of Technology, Minna, Nigeria

[1*]mamudundagi1@gmail.com, [2]mohd.shaba@futminna.edu.ng, [3]aliyumohd@futminna.edu.ng, [4]daniel.peter@futminna.edu.ng, [5]akandetimothy9@gmail.com, [6]adamu.garba@futminna.edu.ng

Abstract

Agricultural crop residues particularly groundnut shell, melon shell and shea nut shell are the main contributors to biomass waste in Nigeria. The mismanagement of these agricultural wastes has become a significant concern causing adverse environmental impacts and also poses a severe threat to soil health. A small capacity (10kg/batch) fixed bed pyrolizer was designed and fabricated for obtaining bio-fuel from these biomasses solid waste. The vertical fixed bed reactor with the dimensions of 600mm length and diameter 150mm was used in carrying out the experiments. The effect of feedstock composition, temperature (200˚C – 500˚C) and residence time (30-120 min) at constant feedstock mass of 500g per run was studied. Three main products were obtained; bio-char, bio-oil and bio-gas. The feedstock composition particle size of 1.18mm was used. The feedstock composition, temperature and residence were found to influence the products yield significantly. The maximum bio-char yield was 72.1 wt% at 200˚C with a residence time of 30 minutes. The maximum bio-oil yield was 43.5 wt% at 500˚C) with a residence time of 120 minutes. The maximum bio-gas yield was 43.4wt% at 500˚C with running time of 120 minutes. Also, the bio-char yield of 39.62 wt%, bio-oil yield of 17.61wt% and bio-gas yield of 41.22wt% at temperature and residence time of 388.07 ˚C and 113.785 minute respectively, resulted in optimum bio-fuel yield having maximum desirability of 1. The reactor efficiency which was evaluated at various temperatures gave maximum efficiency of 60.8%. This indicate that, the reactor is efficient enough to produce bio-oil. Hence, the result obtained contributes to improving mismanagement of agricultural waste that cause adverse environmental impacts.

Keywords: *Pyrolysis, biomass, bio-char, bio-oil and bio-gas.*

1.0 Introduction

More than 700 million Africans use solid biomass fuels, such as wood, charcoal, dung and agricultural residues, for their primary cooking needs. Dependence on solid biomass, especially wood is associated with forest degradation and deforestation, where unsustainable harvesting is practiced. Solid biomass fuels beyond firewood and charcoal can be derived from by-products of agricultural production and forest residues, are becoming increasingly important [1].

The biomass from the agricultural waste, such as rice straw, wheat strew, corn strew, rice husk, groundnut hull, melon hull, shea nut shell and others are all from renewable source. The west African production of shea nut is estimated at 600,000 metric tons per year, while Nigeria accounts for over 50 percent of the production [2]. Nigeria produced about 266.255 metric tons per year of melon hull, and Nigeria is the largest producer of groundnut in Africa and fourth in the world [3] Several groundnut hull, melon hull and shea nut hull are produced from processing these crops, because about half the weight of the seeds are hull [4]. This abundance agricultural wastes show significant environmental pollution. The proper treatment should be applied to the waste (biomass) such as pyrolysis process.

Pyrolysis offers a distinct technology of thermochemical conversion process of biomass. Pyrolysis technologies can be differentiated by the reaction time of the pyrolysis material (slow, intermediate and fast pyrolysis processes) and the heating method [5]. This process occures in the absence of oxgen to transform biomass into different biological and thermochemical product [6]. Depending on the operating condition; pyrolysis can be classified into three main categories: conventional, fast and flash pyrolysis. These differ in process temperature, heating rate, solid residence time and biomass particle size [7]. This process parameters transform biomass into different biofuel products such as; bio-oil, biochar and biogases [8].

Bio-oils are dark, viscous liquid that is made up of highly oxygenated organic compound. Many synonyms of bio-oil include liquid smoke, wood distillates, pyrolysis oils, pyroligneous acid, pyrolysis liquids, bio-crude oil (BCO), wood liquids, wood oil, and liquid wood [7]. Bio-char is another product of the biomass waste pyrolysis, and can be obtained by modifying the pyrolysis system. Bio-char is suitable for use as adsorbents, a precursor of activated carbon, soil amendment, reluctant in the metallurgical industry, and renewable fuel (briquettes) [8].

Received: 03/02/2026; Revised: 17/02/2026; Accepted: 21/02/2026; Published: 11/03/2026

Mismanagement of agricultural waste and traditional disposal method of burning resulting in adverse environmental impacts and poses a severe threat to soil health, disrupting ecosystems and agricultural productivity [9]. This research seeks to develop a pyrolysis system and evaluate its performance for biofuel production

2.0 Materials and Methods

2.1 Materials Collection and Preparation

The materials used for this research work include; galvanized steel, mild steel, copper pipe, electric heater, fiber glass, 0.5HP surface water pump, flange materials, aluminium sheet, bolt and nut, stopwatch, sieve shaker, weighing balance, grinding machine, groundnut shells, melon shells and shear nut shells.

2.2 Design Consideration

The design of the machine (pyrolizer) considers several factors, including the availability and selection of materials, their engineering functionality, component requirements, and overall economical consideration of material cost. Other consideration also includes capacity of the machine (pyrolizer), maintenance, and durability of the machine

2.3 Design of Pyrolysis System

2.3.1 Volume of the reactor

The volume of the reactor was obtained based on the assume capacity of 10 kg/batch of the reactor using Equation (1) [10].

$$V_R = \frac{M}{\rho} \quad (1)$$

Where; V = volume of the reactor, M = mas of the biomass, ϱ = density of the biomass

2.3.2 Height of the reactor

The height of the reactor was obtained using Equation (2) [10]

$$H = \frac{4V_R}{\pi D^2} \quad (2)$$

Where;

H= Height of reactor (cm), V_R = volume of reactor (cm^3); D = assume diameter of the reactor (cm),

2.3.3 Vapour residence time

The vapour residence time of the volatile matter generated while burning the feedstock in a reactor was obtained using Equations 3, 4 and 5 as recommended by [10].

$$\text{Vapour residence time} = \frac{V_r}{V_f} \quad (3)$$

where; V_r = free space in the reactor (cm^3), V_f = volume flow rate (cm^3/min)

$$\text{volume flow rate } V_f = \frac{V_V}{t} \quad (4)$$

where; V_f = volume flow rate (cm^3/min), V_v = volume of volatile and gas generated (cm^3)
t = total time of reactor (min)

$$V_v = \frac{MRT_{ave}}{P} \quad (5)$$

where; M = mass of volatile gases (assumed 60% biomass feed), R = universal gas constant (518.3/kgk), T_{ave} = average operating temperature (°C), P = product volatile and gasses pressure in the reactor (101325 N/m^2)

2.3.4 Design stress

To determine the allowable stress based on the material properties of a mild steel and selected design based on the boiler and pressure vessel British code. The allowable stress is often as fraction of yield strength. Allowable stress was obtained using Equation (6) [11].

$$\delta_{allow} = \frac{\delta_y}{fos} \quad (6)$$

Received: 03/02/2026; Revised: 17/02/2026; Accepted: 21/02/2026; Published: 11/03/2026

Where; δ_y = allowable stress (Mpa or N/mm²), δ_y = yield stress, $fos =$ factor of safety of boiler or pressure vessel

2.3.5 Thickness of Reactor

The thickness of the reactor shell (t) was obtained using Lam's Equation (7) [11].

$$t = \frac{pr}{2\delta_{allow} - p} \quad (7)$$

Where t = thickness of the shell (mm), P= internal reactor pressure (N/mm² or MPa)
r = inner radius of the shell (mm), $2\delta_{allow}$ = design allowable stress (N/mm²)

2.3.6 Insulation thickness

Heat retention in reactor depends on insulation thickness and insulating material used to avoid heat lost through conduction on the walls of the reactor from Equation (8) [11].

$$Q = 2\pi KN(T_p - T_1)/In(R_i - R_p) \quad (8)$$

$$Q/N = 2\pi K(T_p - T_1)/In(R_i - R_p)$$

where; Q = heat loss (W), N = length of pipe (m), Q/N = heat loss per meter of pipe (W/m), T_p = operating of biomass inside a reactor (˚C), T_i = maximum temperature allowed on the outside surface insulation, typically 50 ˚C, R_p = radius of pipe (m), R_i = radius of insulation (m), K = thermal conductivity of insulating material (W/mk).

2.3.7 Design of water-cooled condenser

The condensing process helps to release the latent heat by transferring heat to the surrounding environment. The condenser was design using Equation (9) [12].

$$\Delta T_m = \frac{(T_{v2} - T_{w2}) - (T_{v1} - T_{w1})}{In(T_{v2} - T_{w2})/(T_{v1} - T_{w1})} \quad (9)$$

Where; ΔT_m = mean temperature difference (˚C), T_{w1} = water (inlet temperature (˚C), T_{w2} = water outlet temperature (˚C), T_{v1} = vapour inlet temperature (˚C), T_{v2} = vapor outlet temperature (˚C).
Overall heat transfer between water and vapor was determined using Equation (10) [12].

$$Q = \frac{A \times \Delta_{Tm}}{\frac{1}{h_g} + \frac{\Delta x}{k} + \frac{1}{h}} \quad (10)$$

where; Q = Overall heat transfer (W), A = heat transfer cross sectional area (m²), Δx = thickness of condenser wall (m), K = thermal conductivity of condenser material (W/mk), h_g = enthalpy of gas at operating pressure (kj/kg), h = enthalpy of liquid (kj/kg), ΔT_m = mean temperature difference (°C).

2.4 Biomass Preparation

The collected biomass materials from Paiko town Minna, Niger State shown in Plate I (groundnut shells, melon shells and shea nut shells) were cleaned by removing impurities. The biomass moisture content (15%) was determine using gravimetric method.

Plate I: (a) Groundnut Shells (b) Melon Shells (c) Shea nut Shells

Received: 03/02/2026; Revised: 17/02/2026; Accepted: 21/02/2026; Published: 09/03/2026

The dried biomass was crushed and sieved using 3mm aperture and retained by a 1.18mm sieve aperture to give required size of 1.18mm as shown in Plate II. The pulverized biomass (1.18mm) were weighed and introduced into the reactor. One (1) kg of the samples were weighed and placed inside the reactor for pyrolysis. After each run depending on the residence time the sample are brought out and reweighed. The yield of the biochar was obtained by weighing the quantity of char at the end of the pyrolysis process. While the yield in weight of bio-oil was obtained after the condensation process through the oil collectors. The bio-gas yield was obtained by subtracting the weights of biochar and bio-oil from the weight of the raw biomass.

Plate II: (a) Grounded Groundnut Shells (b) Grounded Melon Shells (c) Grounded Shea nut Shells

2.5 Performance evaluation of the machine using a combined experimental design

The performance evaluation of the machine was carried out using response surface D-optimal design. The experimental design is aimed at evaluating the performance index of the pyrolyzer for biofuel production. The effect of feedstock composition and process parameters on the produced bio-char and bio-oil was evaluated on the biomass pyrolizer. The interaction between composition variables (groundnut shells, melon shells and shea nut shells) and process factors can be better reviewed by experiment that combine mixture components with process factors.

In this work, a (3, 2) simplex lattice mixture design was used for a mixture with three components (groundnut shell, melon shell and shea nut shell). Together with centre point, it has a total of seven runs or seven different combinations as shown in Table 1. A two-level factorial design was used for the two process factors/variables. It has a total of four combinations for these two process factors/variables. The seven different mixtures were made under each of the four process variables combination which gives a total of twenty-eight experimental runs. The two process variables (Temperature and residence time) which are also studied were at two levels each (low and high) as shown in Table 2. using both coded and actual values. Combining the simplex design and the factorial design together gives twenty-eight experimental runs.

Table: 1: (3, 2) Simplex Design Levels

Standard Order	A: Groundnut Shell	B: Melon Shell	C: Shea nut Shell	Response 1: Biochar	Response 2: Bio-oil	Response 3: Bio-gas
1	1	0	0			
2	0.5	0.5	0			
3	0.5	0	0.5			
4	0	1	0			
5	0	0.5	0.5			
6	0	0	1			
7	0.1667	0.1667	0.1667			

Table: 2: Process Variables Levels

Factors	(-) low level	(+) high level
Temperature (°C)	200	500
Residence time (minuts)	120	30

2.6 Model development and optimization of the machine

The effect of temperature and residence time on feedstock composition was estimated based on the quantity of bio-fuel produced using scheffe canonical polynomials, which eliminate the intercept and square terms from the basic models in order to use ordinary least square method for fittings. Proper models by scheffe method for mixture designs including three components consist of linear, quadratic and special interaction models as follows: Linear model.

$$y = b_1x_1 + b_2x_2 + b_3x_3 + e \quad (11)$$

Quadratic model

Received: 03/02/2026; Revised: 17/02/2026; Accepted: 21/02/2026; Published: 11/03/2026

$$y = b_1x_1 + b_2x_2 + b_3x_3 + b_{12}x_1x_2 + b_{13}x_1x_3 + b_{23}x_2x_3 \quad (12)$$

Special interaction model

$$y = b_1x_1 + b_2x_2 + b_3x_3 + +b_{12}x_1x_2 + b_{13}x_1x_3 + b_{23}x_2x_3 + b_{123}x_1x_2x_3 + e \quad (12a)$$

where; x_1 = groundnut shell, x_2 = melon shell, x_3 = shea nut shell

The mixed mathematical model for mixture combined with process factors is obtained by multiplying two models for each part as:

$$Y = F(x)\ Hg\ (z) + e \quad (13)$$

In which y is the response, f(x) indicates a mixture model (scheffe), g(Z) is an ordinary model for the process factors, and e is a random error left out of the fitted model. The best mathematical model was selected according to the comparisons of representative statistical parameters such as standard deviation (SD), coefficient of variation (CV), coefficient of determination (R), adjusted R; and lack of fit test

2.7 Bio-char yield

The bio-char yield is the percentage of bio-char that is present in biofuel after pyrolysis, which was determined using Equation 14 [13].

$$Y_c = \frac{W_{bc}}{W_{ib}} \times 100 \quad (14)$$

Where; Y_c= percentage biochar yield, W_{bc}= weight of biochar (g). W_{ib}= weight of initial biomass(g).

2.8 Bio-oil yield

The bio-oil yield is the percentage of bio-oil present in biofuel after biomass pyrolysis, which was determined using Equation 15 [13].

$$Y_o = \frac{W_{bo}}{W_{ib}} \times 100 \quad (15)$$

Where; Y_o = percentage bio-oil yield,$W_{bo} = \text{weight of bio} - \text{oil (g)}$, W_{ib} = weight of initial biomass(g).

2.9 Bio-gas yield

The bio-gas yield is the percentage of bio-gas present in biofuel after biomass pyrolysis which was determined using Equation 16 [13].

$$\text{Bio-gas yield (\%)} = 100 - (Y_c + Y_o) \quad (16)$$

2.9 Reactor Efficiency

The reactor efficiency was determined using equation (17) [13]. The efficiency of the system in producing biofuel particularly bio-oil was determined at different reactor temperature at which the reactor was tested.

$$\eta_R = \frac{B_{ow} \times B_{oHv}}{W_{bm} \times B_{mHv}} \times 100 \quad (17)$$

Where:

η_R = Reactor Efficiency (%), B_{ow} = Bio-oil weight (kg), B_{oHv} = Bio oil Heating Value (kJ/kg), W_{bm} = Weight of Biomass (kg), B_{mHv} = Biomass heating value (kJ/kg)

3.0 Results and Discussion

3.1 Designed Parameters and the Pyrolysis System

The parameters for the fixed bed pyrolysis machine are shown in Table 3. The pyrolysis machine has reactor volume of 10000 cm^3 this comprises of free space volume of 3000 cm^3 and feedstock volume of 7000 cm^3. The reactor has actual capacity of 9.33 kg/batch. The volatile volume of the machine is indicated by 25.89 cm^3, this value represented the amount of volatile gases a machine can produce by unit volume in cubic meter [14].

The volatile volume of 25.89 cm^3 and volume flow rate of 0.0036 m^3/s are important parameters for calculating vapor residence time. The calculated vapor residence time is approximately 0.83 second as shown in Table 3. This valued is similar to that of [15] study. Vapor residence time in a reactor is an important parameter to achieve maximum yield of liquid. The vapor residence time usually less than 5 seconds for fast pyrolysis otherwise secondary cracking of product would occur resulting in high amount of gas and low amount of liquid production [16].

Received: 03/02/2026; Revised: 17/02/2026; Accepted: 21/02/2026; Published: 09/03/2026

The wall thickness of the reactor obtained was 6.48mm as shown in Table 3, which agreed with the minimum plate thickness as provided in steam broiler code. Reactor diameter of 0.9m or less should have minimum plate thickness of 6mm [11].

For this design specification, the optimal insulation thickness for a reactor was calculated as 96mm as shown in Table 3. The most substantial energy savings are achieved within the initial 50mm of insulation [17].
Adequate heat transfer between water and vapor gives rapid quenching of pyrolysis vapor which promotes high liquid yield [15]. For this design specification, the overall heat transfer between water and vapor was calculated as 92.014W, as shown in Table 3.0. The isometric and the fabricated pyrolysis system are presented in Figure 1 and Plate III respectively.

Table 3: Findings from the Design of Pyrolysis System

S/N	Parameters	Values
1	Capacity of Reactor (kg/hr)	9.33
2	Free Space Volume of Reactor (cm^3)	3000
3	Feedstock Volume (cm^3)	7000
4	Volume of Reactor (cm^3)	10000
5	Volatile Volume (cm^3)	25.89
6	Volume Flow Rate (m^3/s)	0.0036
7	Vapor Residence Time (sec)	0.83
8	Design Stress (N/mm^2)	62. 86
9	Thickness of the Reactor (mm)	6.48
10	Design of Insulator; i. Heat Loss (W/m) ii. Insulation Thickness (mm)	 80 96
11	Design of Cooled Water Condenser; i. Mean Temperature Difference (°C) ii. Overall heat transfer between water and vapor (W).	 174 92.014

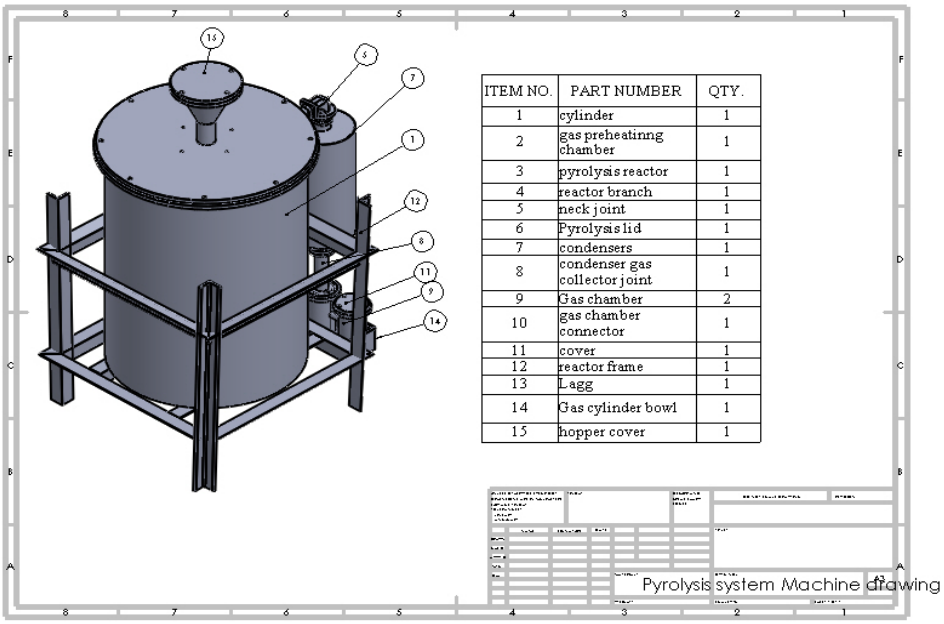

Figure 1: Isometric View of Designed Pyrolyzer

Received: 03/02/2026; Revised: 17/02/2026; Accepted: 21/02/2026; Published: 11/03/2026

Plate III: Fabricated Biomass Pyrolysis System Machine

3.2 Performance evaluation of the machine

3.2.1 Model Adequacy, Factor Effects and Response Surface Interpretation of Biochar Yield

Table 4 shows that the response surface model for biochar yield is highly significant ($F = 81.84$, $p < 0.0001$) with strong goodness-of-fit ($R^2 = 0.9825$; Adjusted $R^2 = 0.9705$) and an adequate signal for optimization (Adeq Precision = 26.42). The low C.V. (4.49%) indicates good experimental precision. However, the pure error is 0.000, meaning replicate variability is essentially absent; therefore, lack-of-fit (LOF) statistics should be interpreted cautiously (LOF is difficult to judge reliably when pure error is near zero). Factor significance indicates that temperature (D) is the dominant driver of biochar yield through strong interaction terms with mixture components (AD, BD, CD all $p < 0.0001$). In contrast, residence time (E) is not significant as a simple two-way interaction with mixture components (AE, BE, CE: $p > 0.05$), but it becomes important through the three-way interaction BDE ($p = 0.0011$), implying residence time affects yield only under specific combinations of groundnut shell fraction (B) and temperature.

Table 4: ANOVA for Response Surface Model Estimated Regression Coefficient and their Effects for Bio-Char Production

Source	**Sum of Squares**	**df**	**Mean Square**	**F-value**	**p-value**	
Model	4839.21	11	439.93	81.84	< 0.0001	Significant
[1]Linear Mixture	1057.98	2	528.99	98.41	< 0.0001	
AD	407.28	1	407.28	75.77	< 0.0001	
AE	0.1210	1	0.1210	0.0225	0.8826	
BD	361.22	1	361.22	67.20	< 0.0001	
BE	15.57	1	15.57	2.90	0.1081	
CD	1244.95	1	1244.95	231.60	< 0.0001	
CE	0.1638	1	0.1638	0.0305	0.8636	
ADE	1.32	1	1.32	0.2464	0.6264	
BDE	83.92	1	83.92	15.61	0.0011	
CDE	3.44	1	3.44	0.6404	0.4353	
Residual	86.00	16	5.38	R^2	0.9825	
Lack of Fit	86.00	11	7.82	Adjusted R^2	0.9705	
Pure Error	0.0000	5	0.0065	Predicted R^2	0.8590	
Cor Total	4925.21	27		Adeq Precision	26.4193	
Std. Dev.	2.32					
Mean	51.64					
C.V. %	4.49					

A: shell butter nut, B: groundnut shell, C: Melon shell, D: temperature, E: residential time

Received: 03/02/2026; Revised: 17/02/2026; Accepted: 21/02/2026; Published: 09/03/2026

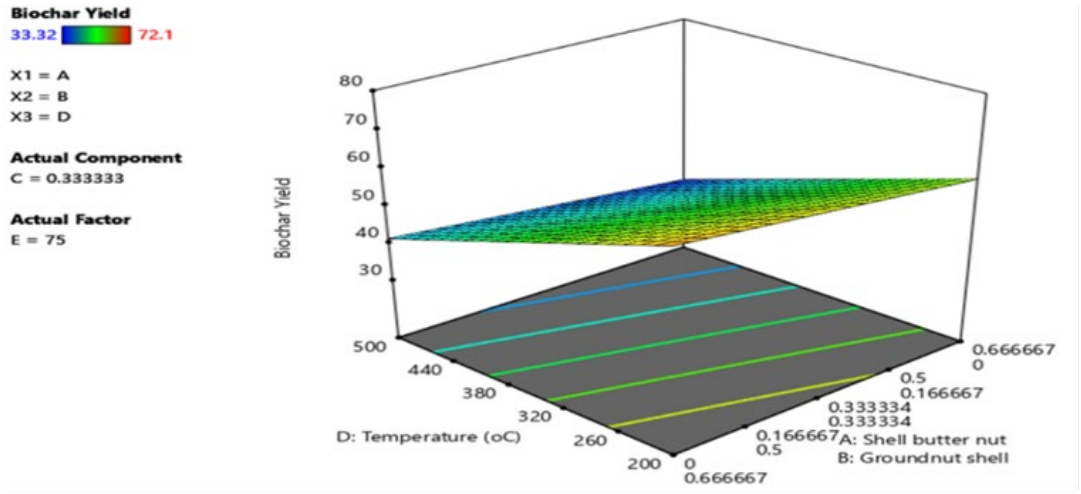

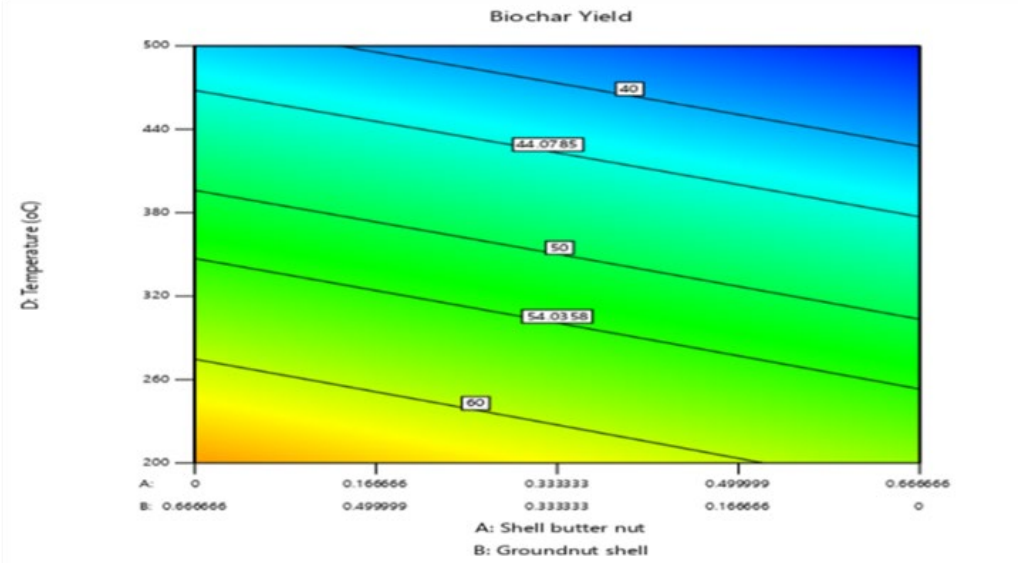

Figure 2: Effects of Feed Stock Composition and Process Variables on Biochar Yield

The 3D surface and contour plots (Figure 2) (at C = 0.3333 and E = 75) show a clear decline in yield as temperature increases (≈ 200 to 500 °C), with yield contours shifting from ~ 60 % at lower temperatures toward ~ 40 % at higher temperatures. This agrees with broad pyrolysis evidence that increasing temperature reduces char yield due to intensified devolatilization and cracking reactions. [18; 19] In terms of magnitude, this study high-temperature yields (~ 40 %) are higher than some single-feedstock groundnut shell studies reporting 30 %, 25 %, and 17 % at 400, 450, and 500 °C, respectively, reflecting how reactor design, heating rate, and yield basis can shift absolute yields. [20] this research temperature-driven decline aligns well with melon seed shell biochar literature showing yields decreasing from 56.60 % to 29.70 % as pyrolysis temperature increases (300 to 450 °C) [21]. Finally, prior work often finds residence time has a smaller effect than temperature across practical ranges, consistent with mostly non-significant time terms except where interactions apply [22].

3.2.2 Model Adequacy, Factor Effects and Response Surface of Bio-oil Production

Table 5 shows that the fitted response-surface mixture model for bio-oil production is statistically robust (Model: F = 75.97, p < 0.0001) with strong explanatory and predictive capability (R^2 = 0.9697; Adj-R^2 = 0.9569; Pred-R^2 = 0.9307) and an adequate signal-to-noise ratio (Adeq Precision = 21.47). The "Linear Mixture" term is significant (p = 0.0002) but contributes a small fraction of variability (SS = 0.0004 vs. Model SS = 0.0080), indicating that composition effects are real yet secondary to process–composition coupling.

Received: 03/02/2026; Revised: 17/02/2026; Accepted: 21/02/2026; Published: 11/03/2026

Table 5: ANOVA for Response Surface Model Estimated Regression Coefficient and their Effects for Bio-oil Production

Source	Sum of Squares	df	Mean Square	F-value	p-value	
Model	0.0080	8	0.0010	75.97	< 0.0001	Significant
[(1)]Linear Mixture	0.0004	2	0.0002	14.45	0.0002	
AD	0.0015	1	0.0015	109.97	< 0.0001	
AE	2.324E-07	1	2.324E-07	0.0176	0.8958	
BD	0.0009	1	0.0009	65.81	< 0.0001	
BE	0.0000	1	0.0000	1.67	0.2115	
CD	0.0025	1	0.0025	192.96	< 0.0001	
CE	2.140E-06	1	2.140E-06	0.1622	0.6916	
Residual	0.0003	19	0.0000	**R^2**	0.9697	
Lack of Fit	0.0003	14	0.0000	**Adjusted R^2**	0.9569	
Pure Error	0.0000	5	0.0000	**Predicted R^2**	0.9307	
Cor Total	0.0083	27		**Adeq Precision**	21.4662	
Std. Dev.	0.0036					
Mean	0.0644					
C.V. %	5.64					

A: shell butter nut, B: groundnut shell, C: Melon shell, D: temperature, E: residential time

This is consistent with Figure 3, where temperature (D) drives the dominant gradient: the contour bands rise from ~14 at ~260 °C to ~16 at ~350 °C, ~18 at ~400 °C, ~20 at ~450 °C and ~22 near ~500 °C, with only slight tilt across the mixture axis. Importantly, Table 4.5 identifies strong mixture–temperature interactions (AD, BD, CD all $p < 0.0001$), confirming that the temperature sensitivity depends on the proportions of shell butter nut (A), groundnut shell (B), and melon shell (C). In contrast, residence time (E) does not significantly interact with any mixture component (AE, BE, CE: $p \geq 0.21$), aligning with the figure's temperature-led pattern and implying that, within the studied domain (e.g., E ≈ 30 min), secondary vapor-phase reactions governed by residence time were not the controlling lever for yield. The observed temperature-dominant behaviour matches recent optimization studies where pyrolysis temperature is repeatedly reported as the primary determinant of bio-oil yield, while residence time often exhibits a weaker marginal effect within practical operating windows [23, 24, 25].

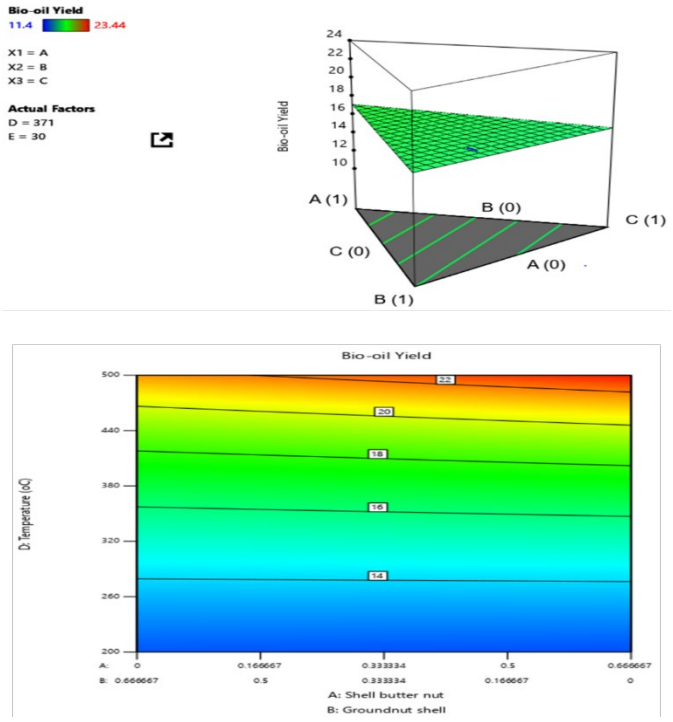

Figure 3: Effects of Feed Stock Composition and Process Variables on Bio-oil Yield

3.2.3 Model Adequacy and Key Process Interactions in the RSM Optimization of Biogas Production.

Table 6 confirms that the bio-gas response surface model is highly significant (Model: F = 107.19, p < 0.0001) with excellent fit (R^2 = 0.9866; Adj-R^2 = 0.9774) and strong signal adequacy (Adeq Precision = 31.60; C.V. = 4.27%). Although Pred-R^2 (0.8751) is lower than Adj-R^2, the gap remains acceptable for process prediction across the design space. The absence of pure error (Pure Error SS = 0) indicates replicate variability was effectively zero, so the lack-of-fit partition (LOF SS = Residual SS = 28.99) not significant because the model's misfit cannot be benchmarked against experimental scatter.

Table 6: ANOVA for Response Surface Model Estimated Regression Coefficient and their Effects for Bio-gas Production

Source	Sum of Squares	Df	Mean Square	F-value	p-value	
Model	2136.13	11	194.19	107.19	< 0.0001	Significant
[(1)]Linear Mixture	721.16	2	360.58	199.04	< 0.0001	
AD	72.72	1	72.72	40.14	< 0.0001	
AE	0.4756s	1	0.4756	0.2625	0.6154	
BD	122.90	1	122.90	67.84	< 0.0001	
BE	17.34	1	17.34	9.57	0.0070	
CD	554.03	1	554.03	305.82	< 0.0001	
CE	0.3509	1	0.3509	0.1937	0.6658	
ADE	0.0913	1	0.0913	0.0504	0.8252	
BDE	57.45	1	57.45	31.71	< 0.0001	
CDE	2.57	1	2.57	1.42	0.2511	
Residual	28.99	16	1.81	**R^2**	0.9866	
Lack of Fit	28.99	11	2.64	**Adjusted R^2**	0.9774	
Pure Error	0.0000	5	0.0000	**Predicted R^2**	0.8751	
Cor Total	2165.12	27		**Adeq Precision**	31.5961	
Std. Dev.	1.35					
Mean	31.53					
C.V. %	4.27					

A: shell butter nut, B: groundnut shell, C: Melon shell, D: temperature, E: residential time

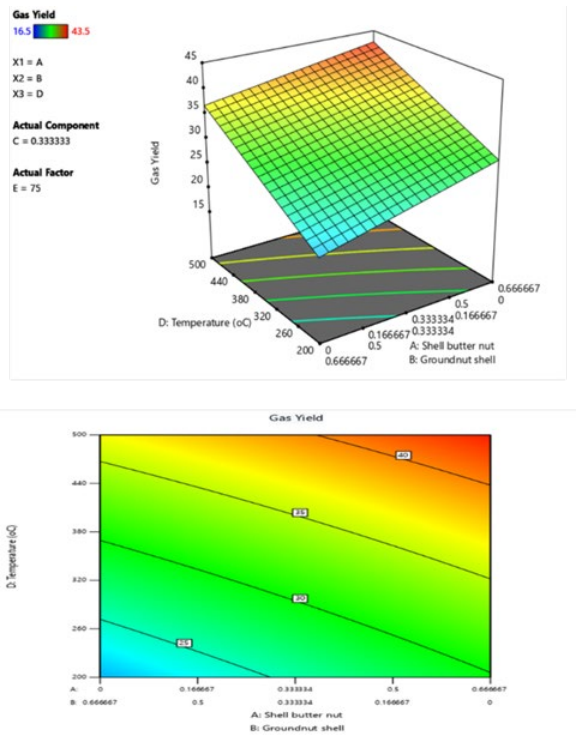

Figure 4: Effects of Feed Stock Composition and Process Variables on Biogas

Process–composition coupling is the dominant driver of gas formation. The linear mixture term is strongly significant (p < 0.0001; SS = 721.16), showing that feedstock proportions materially shift gas yield. Among

interaction effects, temperature coupling is strongest with component C (CD: SS = 554.03; F = 305.82; $p < 0.0001$), followed by BD (SS = 122.90) and AD (SS = 72.72), establishing that the temperature sensitivity depends on mixture identity—consistent with literature that secondary cracking and devolatilization pathways vary with biomass composition and ash/mineral catalysis [26; 27]. Residence-time effects are selective: BE is significant ($p = 0.0070$) while AE and CE are not, and only the three-way interaction BDE is significant ($F = 31.71$; $p < 0.0001$). This pattern implies that, at specific temperatures, longer residence time amplifies gas production preferentially in blends richer in groundnut shell (B), plausibly via enhanced secondary cracking of condensable vapors to permanent gases—an effect widely attributed to increased vapor-phase reaction opportunity at longer gas residence/retention [28, 29].

Figure 4 (C fixed at 0.3333; E = 75) visually corroborates Table 4.6: gas yield increases monotonically with temperature from the blue/green region (~25 at ~260 °C) through ~30 (≈320 °C), ~35 (≈390–400 °C), to ~40 near ≈460–480 °C, reaching the maximum zone (~43.5) at the highest temperature and highest A fraction (A ≈ 0.6667; B ≈ 0). The diagonal contour tilt indicates a secondary but consistent composition effect: increasing A (and decreasing B) elevates gas yield at any fixed temperature, while temperature remains the principal gradient—consistent with RSM-based thermochemical optimization studies where mixture terms and operating parameters jointly govern gas yield [30].

3.3 Numerical Optimization Results and Desirability Evaluation for Balanced Yields of Biochar, Bio-Oil, and Biogas in the Pyrolysis Process.

Table 7 defines a multi-response numerical optimization in which all mixture components (A to C) are constrained to feasible proportions (0 to 1), while operating variables are bounded at 200 to 500 °C (D) and 30 to 120 min (E). All five factors carry identical settings (weights = 1; importance = 3), so the optimizer is structured to search a balanced optimum rather than privileging any single factor. Likewise, the three responses are simultaneously set to maximize within observed experimental ranges: biochar (33.32 to 72.10%), bio-oil (11.40 to 23.44%), and biogas (16.50–43.50%).

Table 7: Constraints for Numerical Optimization for Bio-Fuel Production

Name	Goal	Lower Limit	Upper Limit	Lower Weight	Upper Weight	Importance
A: Shell butter nut	is in range	0	1	1	1	3
B:Groundnut shell	is in range	0	1	1	1	3
C:Melon shell	is in range	0	1	1	1	3
D:Temperature	is in range	200	500	1	1	3
E:Residential time	is in range	30	120	1	1	3
Biochar Yield	maximize	33.32	72.1	1	1	3
Bio-oil Yield	maximize	11.4	23.44	1	1	3
Gas Yield	maximize	16.5	43.5	1	1	3

Table 8 reports the top-ranked solution (No. 1) at A = 1.0, B = 0, C = 0, with D = 388.007 °C and E = 113.785 min, predicting 39.620 % biochar, 17.61 % bio-oil, and 41.22 % biogas. These predicted yields are all inside the imposed bounds, but they are not simultaneously near the upper limits—notably, biochar remains relatively low compared with its allowable maximum (72.10 %), whereas biogas approaches its upper bound (43.50 %). This pattern indicates an inherent trade-off surface in the fitted models: conditions that push biogas upward (higher severity) typically do not co-maximize char and oil, and numerical optimization therefore identifies a compromise point rather than a boundary solution, consistent with RSM optimization studies that report competing objectives among pyrolysis product fractions [31].

Table 8: Numerical Optimization Parameters

Number	Shearnut shell (%)	Groundnut shell (%)	Melon shell (%)	Tempt (^oC)	Resident Time (min)	Biochar Yield (%)	Bio oil yield (%)	Biogas yield (%)	Desirability
1.	1	0	0	388.007	113.785	39.620	17.61	41.22	1

Received: 03/02/2026; Revised: 17/02/2026; Accepted: 21/02/2026; Published: 09/03/2026

Figure 5 clarifies how this compromise is scored under the desirability framework. The factor desirabilities for A to E are all 1.0 (blue bars), confirming the solution sits entirely within the specified factor ranges. However, the response desirabilities differ substantially: bio-oil = 0.954, biogas = 0.503, and biochar = 0.402, yielding a combined desirability = 0.578 (Solution 1 of 19). Because overall desirability is computed by combining individual desirability on a 0 to 1 scale (commonly via a geometric aggregation), moderate desirability for any response depresses the combined score even when another response (bio-oil here) is near-optimal. This explains why the selected operating point strongly favors high bio-oil satisfaction while accepting mid-range satisfaction for biogas and biochar—an outcome aligned with recent multi-criteria pyrolysis optimization practice where desirability is used explicitly to manage product-distribution trade-offs [32].

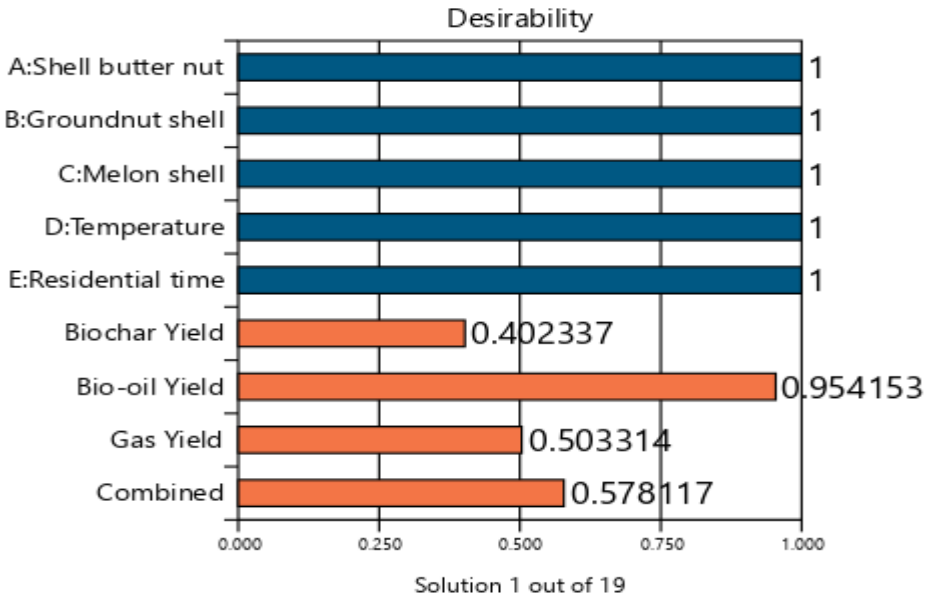

3.4 Efficiency Evaluation of the Pyrolysis Reactor

A graph of the reactor efficiency was plotted with the varying reactor temperature (Figure 6). The graph shows the efficiency of the reactor in generating bio-oil increase to 60.8% maximum at temperature of 500 ˚C. However, the efficiency was decreasing at temperature above 500 ˚C because the weight of the bio-oil generated was low. At the end an overall average of 62.42% efficiency was achieved for the reactor.

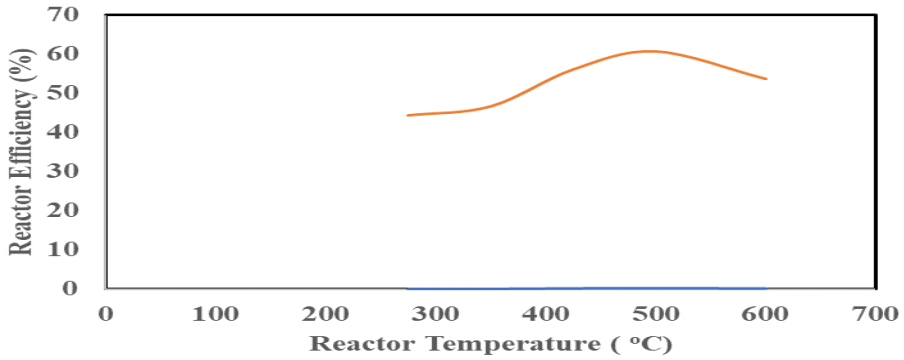

Figure 6: Variation of Reactor Efficiency with Reactor Temperature

5. Conclusion

In this study a fixed bed pyrolysis system was developed and evaluated with actual capacity of 9.33kg/h. The major components of the biomass pyrolysis machine include the reactor, condenser, oil collections, char discharge assembly, heating elements housing. The performance of the pyrolyzes has maximum yields of 72.1wt %, 43.5wt %, 43.4 % biochar, bio-oil of and biogas respectively at particle size of feedstock 1.18mm, temperature of 500 ˚C and residence time of 120 minutes. The efficiency of the fixed bed pyrolysis system to yield maximum and minimum biofuel was evaluated to be 60.8% (at 500 ˚C) and 50.5 % at (at 600 ˚C) respectively.

Hence, the study contributes to improving mismanagement of agricultural waste and traditional disposal method of burning, that cause adverse environmental impacts owing to the high efficiency of the developed a pyrolizer.

References

Received: 03/02/2026; Revised: 17/02/2026; Accepted: 21/02/2026; Published: 11/03/2026

[1] Japhet, J. A., Luka, B. S., Maren, I. B., and Datau, S. G. (2020). The potential of wood and agricultural waste for pellet fuel development in nigeria—A technical review. *Int. J. Eng. Appl. Sci. Technol*, *4*, 598–607.

[2] Eneh, M. C. C. (2010). An overview of shea nut and shea butter industry in Nigeria. *National Seminal Organized by Central Bank of Nigeria in Collaboration with Federal Ministry of Agriculture and Rural Development and Nigeria Export Promotion Council (Nepc) Niger State*, 1–4.

[3] Opeke, L. K. (2006). Essential of crop farming. Spectrum Book Limited. *Spectrum House Ring Road, Ibadan*, 81–84.

[4] Grubben, G. J. H. and Denton, O. A (Editors) (2019). PROTA (plant resources of Tropical Africa, wagenningen, Netherlands) Accessed is September, 2023.

[5] Antal, M. J., and Grønli, M. (2003). The art, science, and technology of charcoal production. *Industrial & Engineering Chemistry Research*, *42*(8), 1619–1640.

[6] Zhang, H., Luo, M., Xiao, R., Shao, S., Jin, B., Xiao, G., Zhao, M., and Liang, J. (2014). Catalytic conversion of biomass pyrolysis-derived compounds with chemical liquid deposition (CLD) modified ZSM-5. *Bioresource Technology*, *155*, 57–62.

[7] Balat, M. (2011). An overview of the properties and applications of biomass pyrolysis oils. *Energy Sources, Part A: Recovery, Utilization, and Environmental Effects*, *33*(7), 674–689.

[8] Shen, Y., Ma, D., and Ge, X. (2017). CO 2-looping in biomass pyrolysis or gasification. *Sustainable Energy & Fuels*, *1*(8), 1700–1729.

[9] Mohammed, I. S., Na, R., Kushima, K., and Shimizu, N. (2020). *Investigating the effect of processing parameters on the products of hydrothermal carbonization of corn Stover. Sustainability 12: 5100*.

[10] Ogunkanmi, J. O., Kulla, D. M., Omisanya, N. O., Sumaila, M., Obada, D. O., and Dodoo-Arhin, D. (2018). Extraction of bio-oil during pyrolysis of locally sourced palm kernel shells: Effect of process parameters. *Case Studies in Thermal Engineering*, *12*, 711–716.

[11] Khurmi, R. S., and Gupta, J. K. (2005). *A textbook of machine design*. S. Chand publishing.

[12] Rajput, R. K. (2012). Heat and mass transfer (8th Edition): Laxmi Publications Limited, 113 Golden House, Daryaganj, New Delhi, pp 503-527

[13] Akinola, A. O., and Vol, T. (2016). Evaluation of the efficiency of a thermochemical reactor for wood pyrolysis. *European Journal of Engineering and Technology* *4*(4).

[14] Usiabulu, G. I., Ogbonna, J., Aimikhe, V., Okafor, E., and Nosike, L. (2023). Estimation of Gas leak volume to quantify gaseous fluid flow in processing plants. *Journal of Applied Sciences and Environmental Management*, *27*(8), 1761-1769.

[15] Hossain, A., Hasan, R., and Islam, R. (2014). Design, fabrication and performance study of a biomass solid waste pyrolysis system for alternative liquid fuel production. *Global J Res Eng*, *14*, 25–34.

[16] Bridgwater, A. V. (2012). Review of fast pyrolysis of biomass and product upgrading. *Biomass and Bioenergy*, *38*, 68–94. https://doi.org/10.1016/j.biombioe.2011.01.048

[17] Zhao, C., Jiang, E., and Chen, A. (2017). Volatile production from pyrolysis of cellulose, hemicellulose and lignin. *Journal of the Energy Institute*, *90*(6), 902–913.

[18] Altıkat, A., Alma, M. H., Altıkat, A., Bilgili, M. E., and Altıkat, S. (2024). A comprehensive study of biochar yield and quality concerning pyrolysis conditions: A multifaceted approach. Sustainability, 16(2), 937.

[19] Khater, E. S., Bahnasawy, A., Hamouda, R., Sabahy, A., Abbas, W., and Morsy, O. M. (2024). Biochar production under different pyrolysis temperatures with different types of agricultural wastes. *Scientific Reports*, *14*(1), 2625.

[20] Tomczyk, A., Sokołowska, Z., and Boguta, P. (2020). Biochar physicochemical properties: pyrolysis temperature and feedstock kind effects. *Reviews in Environmental Science and Bio/Technology*, *19*(1), 191-215.

[21] Pawar, A., & Panwar, N. L. (2022). Experimental investigation on biochar from groundnut shell in a continuous production system. *Biomass Conversion and Biorefinery*, *12*(4), 1093-1103.

[22] Zhao, B., O'Connor, D., Zhang, J., Peng, T., Shen, Z., Tsang, D. C., and Hou, D. (2018). Effect of pyrolysis temperature, heating rate, and residence time on rapeseed stem derived biochar. *Journal of Cleaner Production*, *174*, 977-987.

[23] Kaur, L., Singh, J., Ashok, A., and Kumar, V. (2024). Design expert based optimization of the pyrolysis process for the production of cattle dung bio-oil and properties characterization. *Scientific Reports*, *14*(1), 9421.

[24] Ikpeseni, S. C., Sada, S. O., Efetobor, U. J., Orugba, H. O., Ekpu, M., Owamah, H. I., ... and Onochie, U. P. (2024). Optimization of bio-oil production parameters from the pyrolysis of elephant grass (Pennisetum purpureum) using response surface methodology. *Clean Energy*, *8*(5), 241-251.

[25] Kumar Mishra, R., and Vinu, R. (2024). Pyrolysis characteristics and kinetic investigation of waste groundnut shells using thermogravimetric analyzer, Py-FTIR, and Py-GC-MS. *Journal of Analytical and Applied Pyrolysis, 173*, 106514.

Received: 03/02/2026; Revised: 17/02/2026; Accepted: 21/02/2026; Published: 09/03/2026

[26] Zhang, Y., Liang, Y., Li, S., Yuan, Y., Zhang, D., Wu, Y., Xie, H., Brindhadevi, K., Pugazhendhi, A., and Xia, C. (2023). A review of biomass pyrolysis gas: Forming mechanisms, influencing parameters, and product application upgrades. Fuel, 347, 128461. https://doi.org/10.1016/j.fuel.2023.128461

[27] Mishra, R. K., and Vinu, R. (2024). Pyrolysis characteristics and kinetic investigation of waste groundnut shells using thermogravimetric analyzer, Py-FTIR, and Py-GC-MS. Journal of Analytical and Applied Pyrolysis, 179, 106514. https://doi.org/10.1016/j.jaap.2024.106514

[28] Li, X., Wu, S., Xing, X., Zhou, T., and Zhao, Y. (2025). *Evolution mechanisms of gas-solid products in multi-source sludge pyrolysis: Synergistic regulation by temperature and time parameters*. Sustainability, 17(22), 10270. https://doi.org/10.3390/su172210270

[29] Morvaridi, R., Hallajisani, A., and Rasouli, J. (2025). Effect of temperature and type of catalyst on the composition of pyrolysis oil obtained from oil sludge. Journal of Material Cycles and Waste Management, 27, 2269–2285.

[30] Viswakethu, C., Pichappan, R., Perumal, P., and Lakshmaiya, N. (2024). An experimental and response-surface-based optimization approach towards production of producer gas in a circulating fluidized bed gasifier using blends of renewable fibre-based biomass mixtures. **Sustainable Energy** and **Fuels, 8**, 975–986. https://doi.org/10.1039/D3SE00551H

[31] Saikia, S., and Kalamdhad, A. S. (2023). Response surface methodology (RSM)-based pyrolysis process parameter optimization for char generation from municipal solid waste (MSW) in a fixed bed reactor. *Sustainable Energy Technologies and Assessments*, *60*, 103541.

[32] Mariyam, S., Alherbawi, M., McKay, G., and Al-Ansari, T. (2025). A predictive model for biomass waste pyrolysis yield: Exploring the correlation of proximate analysis and product composition. *Energy Conversion and Management: X*, *25*, 100831.

Received: 03/02/2026; Revised: 17/02/2026; Accepted: 21/02/2026; Published: 11/03/2026